ELSEVIER

Chemical Engineering Science 61 (2006) 3496–3505

Chemical Engineering Science

www.elsevier.com/locate/ces

Spin and dip coating of light-emitting polymer solutions: Matching experiment with modelling

P. Yimsiri[a,*], M.R. Mackley[b]

[a]Department of Chemical Engineering, Faculty of Engineering, Burapha University, Chonburi 20131, Thailand
[b]Department of Chemical Engineering, University of Cambridge, UK

Received 8 July 2005; received in revised form 27 November 2005; accepted 17 December 2005
Available online 7 February 2006

Abstract

This paper reports experimental observations on spin and dip coating of light-emitting polymer (LEP) solutions where both the process conditions as well as the solution properties are factors influencing thickness and uniformity of thin LEP films. In terms of spin coating, which is a typical process for the manufacture of polymer light-emitting diodes (PLEDs), a number of process variables including spin speed were systematically explored. A matching series of dip-coating experiments was also carried out with the retraction speed as a primary variable. Modifications of existing models for both spin and dip coating were developed to include solvent evaporation and the effect of solution viscosity change during evaporation. Both models were found to give reasonable agreement with the major observed trends for final film thickness as a function of process conditions tested in this paper.

Keywords: Spin coating; Dip coating; Light-emitting polymer; Thin film; Polymer light-emitting diode; Nanostructure

1. Introduction

Light-emitting polymers (LEPs) are now well established as potential devices for the manufacture of optical display technology (see, for example, Burroughes et al., 1990; Mentley, 2002; Chou et al., 2005) and a key feature of a polymer light-emitting diode (PLED) is the necessity to produce a solid thin LEP film sandwiched between two electrodes. A device can be fabricated as shown in Fig. 1 using a glass substrate support where indium tin oxide (ITO) is commonly used as a transparent anode that is coated on the glass substrate by electron-beam evaporation or sputtering (Braun and Heeger, 1991; Wu et al., 1997; Kim et al., 1999). A typical device then consists of two polymer layers. The first layer spin coated onto the anode (thickness of around 500 Å) is non-emissive and its primary, but not necessarily only, function is to aid hole-injection properties. Poly(3,4-ethylenedioxythiophene), PEDT, doped with Polystyrene Sulphonic acid (PSS) was chosen in this study. It cannot emit light due to a very small band gap of 1.6 eV ($\lambda = 775$ nm) which is in an infrared region (Sapp et al., 1998). A thin LEP film, which is the emissive layer, is prepared by spin coating a polymer solution on top of the PEDT:PSS layer and it is this process that this paper is concerned with. Typically, the film thickness needs to be of order of 700–1000 Å (Kim et al., 1999; Carter et al., 1997). A layer of calcium/aluminium is then deposited on the 'top' surface by thermal evaporation. If an electric field is applied across the device, the device can emit in either the red, green, or blue regime depending on the band gap of the polymers that have been used.

An extensive range of LEPs has now been reported in the scientific literature (see, for example, Janietz et al., 1998; Redecker et al., 1998; Stevens et al., 2001). In this paper, a limited range of LEPs were used and their properties are described in Section 2.

An important characteristic of PLEDs is their ease of manufacturing when compared to small organic molecule light-emitting diodes (OLEDs) and traditional inorganic LEDs, both of which have crystalline structures that are grown under vacuum conditions using costly equipment. By contrast the

* Corresponding author. Tel.: +66 3874 5900x3351; fax: +66 3874 5900x3350.
E-mail address: pyimsiri@buu.ac.th (P. Yimsiri).

0009-2509/$ - see front matter © 2006 Elsevier Ltd. All rights reserved.
doi:10.1016/j.ces.2005.12.018

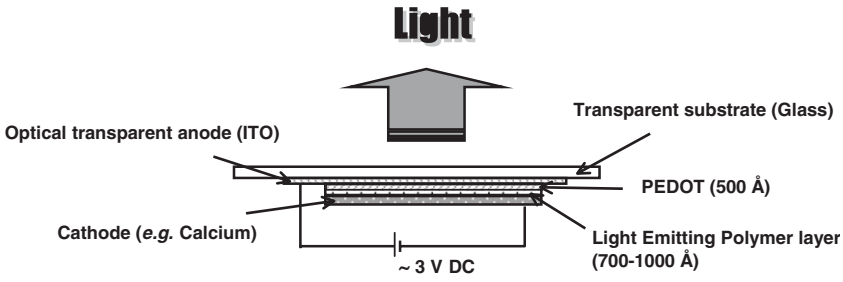

Fig. 1. Basic structure of PLEDs.

manufacturing process of PLEDs is relatively simple. In order to manufacture PLEDs, it is necessary to prepare a uniform thin film of LEP and this is normally carried out using the spin-coating process, transforming a low-viscosity liquid polymer solution into a solid LEP film (Carter et al., 1997; Friend et al., 1999). Spin coating is a well-established technology which in the past has been used in the manufacture of photoresists and oxide coatings for screens (Emslie et al., 1958; Hall et al., 1998). There is a substantial scientific literature on the spin-coating process and useful reviews on the subject are given by Scriven (1988) and Larson and Rehg (1997). Of particular relevance to this paper is the work of Emslie et al. (1958) who established how a Newtonian fluid thins under the action of a centrifugal rotation on a flat disc. His model described the importance of spin speed, liquid viscosity, and spin time on the film thickness.

The dip-coating process was first commercially used to produce thin films in a sol–gel technology in 1939 (Brinker and Hurd, 1994). It has also been used to produce thin films in other technologies, such as photoresists films (Gibson et al., 1985) and lubricant layers for magnetic hard disks (Gao et al., 1995). Dip coating is a simple process for depositing a thin film of solution onto a plate, cylinder, or irregular-shaped object. The fact that the geometry of the substrates can vary widely is a distinguishing feature of the dip-coating technique. The process involves immersing a substrate into a reservoir of solution for some time thereby ensuring that the substrate is completely wetted, and then withdrawing the substrate from the solution bath. The liquid film formation is achieved by two main mechanisms, i.e. gravity draining of liquid solution and evaporation of solvent. An early dip-coating analysis was presented by Landau and Levich (1942). This model is a 1-D model derived purely from hydrodynamics of a Newtonian fluid flow, ignoring solvent evaporation.

In this paper, a series of experiments was carried out for a range of LEP solutions for both spin and dip coating. In both cases, models were modified and compared with the experimental results. In the following section, the polymer solutions and their rheology are given. The experimental results for spin coating are then reported, followed by the spin-coating models. The experimental dip-coating data is then presented followed by its respective model. Finally, conclusions for the overall work are given.

2. LEP solutions and rheological characterisation

The LEP solutions used were blends of two different LEP systems, namely poly(9,9-dioctylfluorene-*co*-benzothiadiazole) (F8BT) and poly(9,9-dioctylfluorene-*co*-TFB) (Host 1), with a weight ratio of approximately 5:95. Details of the LEP solutions used in this paper are shown in Table 1.

Rheological characterisation of LEP solutions was carried out in order to establish how polymer solution rheology influenced thin film processing. A Rheometrics Dynamic Spectrometer (RDS II), a strain-controlled rotational rheometer, was used in order to obtain the magnitude of solution viscosity. The RDS II measures the torque response and converts to shear stress as the sample is subjected to prescribed shear deformations. The characterisation was performed at 20 °C controlled by an ethylene glycol bath and in a range of shear rates equivalent to spin speeds between 500–5000 rpm. In addition, different solution concentrations (up to 10% w/v due to a very low solubility of the LEPs in xylene) were carried out in order to accomplish the change in viscosity with concentration as the thin film dries. This information was useful for the subsequent modelling of thin films. Fig. 2 shows that the solution viscosities in the ranges of concentration 0.5–10% w/v are essentially Newtonian, i.e. the viscosity is independent of shear rate. The relationship between the Newtonian viscosity and concentration of the solutions given in Fig. 3 shows that the viscosity increases to a first approximation exponentially with the increase in concentration and the data followed the "Martin equation" (Macosko, 1994). From the results shown here it can be concluded that at low initial spinning concentrations the fluid is essentially Newtonian, with a low viscosity. As solvent evaporation proceeds during the drying process of the film, the viscosity substantially rises.

Table 1
Details of LEP solutions

Solution	Concentration (% w/v)	Solvent	Newtonian viscosity (Pa s)	M_w of F8BT (M_w of Host 1 = 95,000)
1	1.6	Xylene	2.5×10^{-3}	151,000
2	3.0	Xylene	8.5×10^{-3}	151,000
3	1.6	Xylene	1.8×10^{-3}	61,400
4	1.6	Xylene	2.5×10^{-3}	504,000

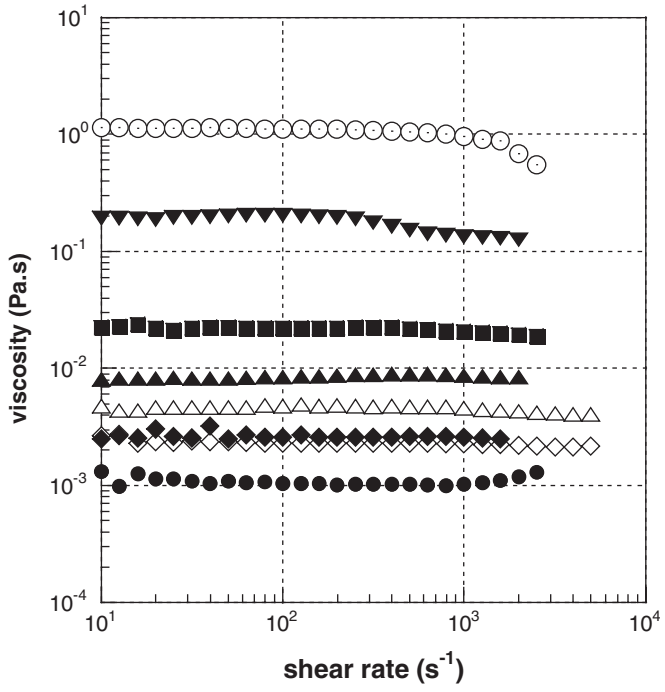

Fig. 2. Viscosities of solution 1 at various concentrations: (●) 0.5%, (◇) 1%, (◆) 1.6%, (△) 2%, (▲) 3%, (■) 5%, (▼) 8%, and (◯) 10% w/v.

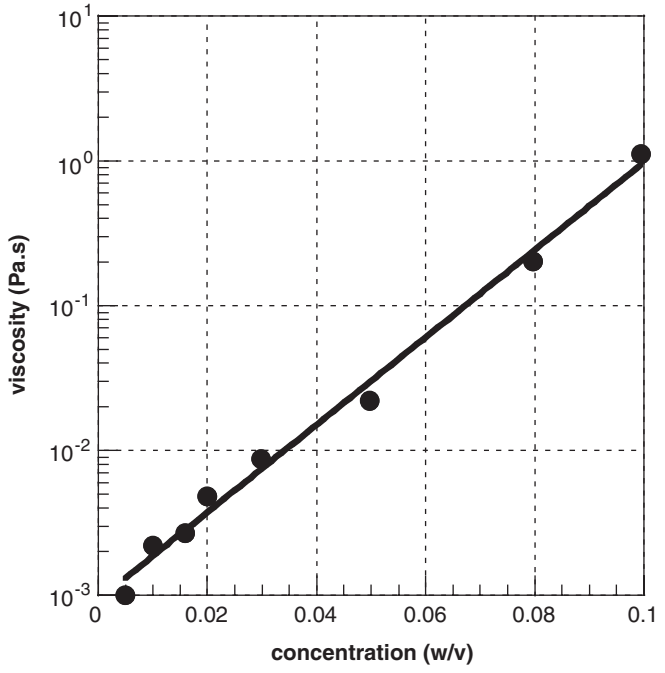

Fig. 3. Relationship between viscosity and concentration of solution 1: Closed circles: experimental data, continuous line: exponential fitting.

3. Experimental procedure: spin coating

The LEP thin films were prepared using a commercial ITO-coated glass substrates of sizes 25×25 and 50×50 mm^2, both 1 mm thick. The substrates were cleaned using THF, rinsed with a mixture of isopropanol and water, and dried using filtered dry nitrogen gas. The spin coater used was a Karl Suss RC 8 GYRSET, which can operate with a rotating cover called a GYRSET. The GYRSET system is a closed chamber that creates a solvent-rich environment above the substrate. The evaporation rate of the polymer solution can thus be controlled by the use of the GYRSET. The spinning with GYRSET is henceforth referred to as 'slow evaporation' whereas the spinning without GYRSET is referred to as 'fast evaporation'. An initial acceleration of 500 rpm/s and a spin time of 60 s were used throughout the experiments. It was found that in most cases film thickness was essentially independent of time providing a minimum spin time of 40 s was used.

Once the thin LEP film has been produced, the film thickness was measured using a surface profilometer, Veeco Dektak 3. In order to measure the film thickness, the sample was scratched with a groove using a scalpel. Measurements were made electronically by moving the sample beneath a diamond-tipped stylus at a setting scan length and speed. As the stage moves, the stylus, which is mechanically coupled to the core of an linear variable differential transformer (LVDT), rides over the sample surface. Surface variations (level differences between the surface of the film and the surface of the substrate) cause the stylus to be translated vertically, resulting in changing the core position of the LVDT. Electrical signals produced by the LVDT are sent to the computer analyser and converted to a digital format through a high precision, integrating analogue to digital converter.

4. Spin-coating experimental results

Fig. 4 shows the effect of spin time for a specific set of conditions and the results show that provided the spin time is greater than approximately 40 s the thickness of the film is essentially independent of time. In all further cases, a spin time of 60 s was used.

Fig. 5 presents measured film thickness as a function of spin speed, solvent evaporation rate, and polymer concentration. For both fast and slow evaporation, the film thickness decreases with increasing spin speed, ω, due to the increase in the centrifugal forces associated with the rotary motion. The higher force creates more liquid outflow resulting in a thinner film. However, for fast solvent evaporation the film thickness reaches a plateau stage at high spin speeds as seen from the results of solution 2 at the spin speed of 1500 and 3000 rpm. These results agree with similar experimental findings of Schwartz (1965), Damon (1966) and Hall et al. (1998).

The relationship between the film thickness and spin speed was found to be a power law of the form $h \propto \omega^{-b}$ (e.g. Emslie et al., 1958; Meyerhofer, 1978) where b was experimentally found to be in a range of 0.4–0.9 in this study. The small value of b of 0.41 was found for the case of solution 2 spinning without the GYRSET.

In terms of the solvent evaporation rate, the results show that the films prepared without GYRSET (fast evaporation) are thicker than those prepared with the GYRSET (slow evaporation). This is because as the solvent evaporates during the

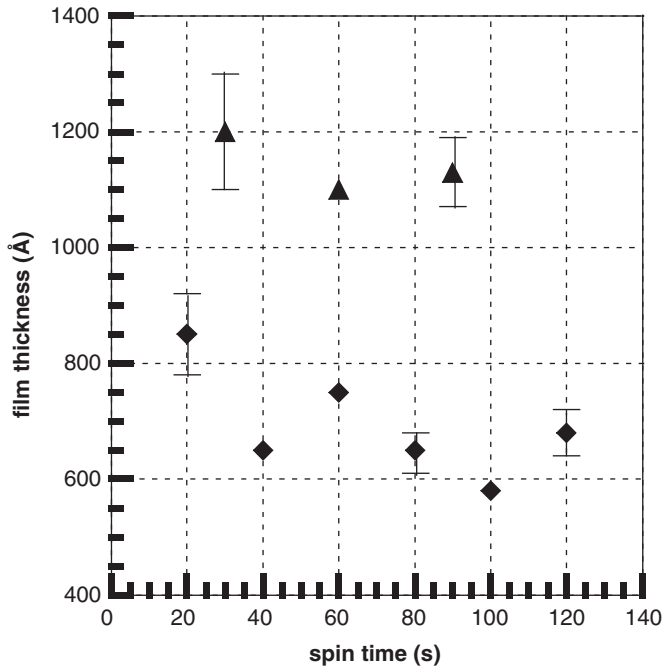

Fig. 4. Film thickness as a function of spin time. Spin with GYRSET (slow evaporation): (♦) solution 1 and (▲) solution 2.

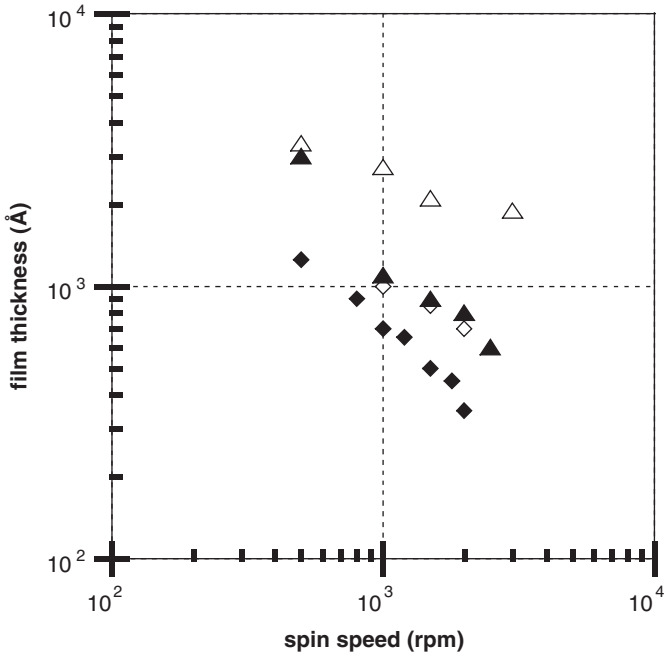

Fig. 5. Film thickness as a function of spin speed. Spin without GYRSET (fast evaporation): (◇) solution 1 ($b = 0.75$) and (△) solution 2 ($b = 0.33$). Spin with GYRSET (slow evaporation): (♦) solution 1 ($b = 0.58$) and (▲) solution 2 ($b = 0.94$).

spinning, the solution concentration increases and hence, the solution viscosity also increases and this retards the film thinning process.

Results reveal that a solution with a higher initial concentration produces thicker films for both fast and slow evaporation

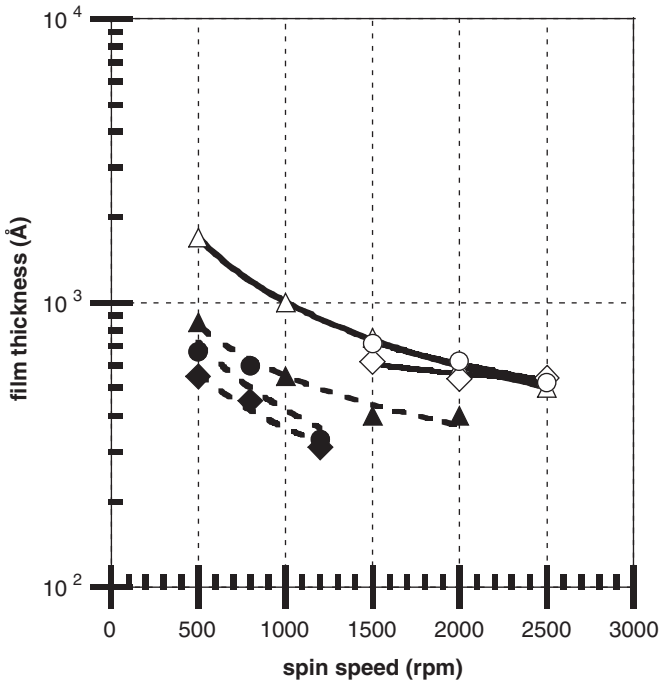

Fig. 6. Effect of starting solution viscosity on the film thickness. Spin without GYRSET (fast evaporation): (△) solution 1, (◇) solution 3, and (◯) solution 4. Spin with GYRSET (slow evaporation): (▲) solution 1, (♦) solution 3, and (●) solution 4.

when compared with a lower concentration solution. The dependency of the solution concentration on film thickness was also reported in previous studies (e.g. Extrand, 1994; Gupta and Gupta, 1998; Hall et al., 1998). Damon (1966) combined the effects of viscosity and concentration into an empirical correction between the film thickness and solution concentration, c, which was in a form of $h \propto c^2$.

In order to vary an initial LEP solution viscosity, different molecular weight of F8BT and Host1 were used. Solutions 1, 3, and 4 were all prepared using xylene as a solvent and had the same concentration of 1.6% w/v. The effect of solution concentration was linked with the effect of solution viscosity by some researchers (Damon, 1966; Schwartz, 1965; Weill and Dechenaux, 1988). In their experiments, different viscosity solutions were obtained by varying the concentration of the same material. This method is only applicable for non-volatile solutions. For a volatile system, the variation of the solution viscosity should be achieved by using different molecular weight polymers to exclude the effect of solution concentration.

For fast evaporation, the results presented in Fig. 6 fall onto one trend line. The films produced from most solutions show a slight difference in the thickness, indicating a weak influence of the viscosity on the film thickness. For slow evaporation, the trend lines do not overlap, implying that the film thickness depends on the viscosity of the solutions. As the viscosity increases, the thickness of the film increases. The thickness dependency on the solution viscosity was also reported by Daughton et al. (1978) although they did not clearly explain if the effect of viscosity was due to the effect of

concentration. It can be concluded that the effect of the initial viscosity is dependent on the solvent evaporation. If the solvent evaporation is the main mechanism in the film thinning, the viscosity of the solution does not play a significant role, and vice versa.

5. Modelling of spin-coating process

The earliest spin-coating model was developed by Emslie et al. (1958) where a one-dimensional model was derived from a balance between rotational centrifugal forces and viscous shear forces with assumptions of (i) radially symmetric flow, (ii) a Newtonian fluid, and (iii) negligible edge effects, Coriolis and gravitation forces. The advantage of the model is its simplicity but yet an ability to predict film thickness trends. However, the effect of solvent evaporation was not considered in the model and hence, a disadvantage in the context of this work where volatile solvents were used.

Meyerhofer (1978) further developed Emslie's model by taking into account the effects of solvent evaporation. The concept of his analytical model is that the film thinning is a result of two sequential mechanisms, i.e. the convective radial outflow and the solvent evaporation. Initially, liquid thins down due to the radial outflow driven by the centrifugal force. At this stage, the solvent evaporation is negligible. As the liquid thins down, the rate of the radial outflow decreases and the solvent evaporation dominates the film thinning.

A modified model, which is a combination of Emslie's model and a two-stage solvent evaporation, is proposed in this paper. The concept of the model is that the film thinning is a result of two mechanisms (see Fig. 7), i.e. the convective radial outflow and the solvent evaporation. During the first stage, the liquid thinning is a result of both mechanisms, not only the radial flow as suggested by Meyerhofer (1978). As the solvent is lost by the evaporation, the concentration of the solution increases and therefore the viscosity of the solution also increases. The change of the solution viscosity with the concentration is taken into account in the modified model. A second stage is assumed to start when the solution concentration reaches a critical value (say 10% w/v). The concentration of 10% w/v represents a maximum concentration of LEPs dissolved with xylene and this value was found from experiments in this study. Although the critical concentration depends on molecular weight of the LEPs, there is no significant difference in the values. At this stage, we assumed that the material can no longer radially flow outwards and further thinning occurred by solvent evaporation only.

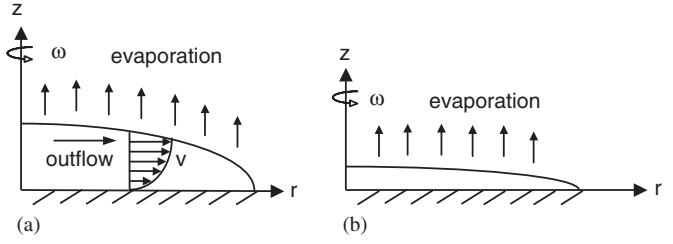

Fig. 7. Schematic diagram of liquid thinning in spin-coating process: (a) first stage and (b) second stage.

It was assumed that during the first stage, the film thinning mechanism involves both radially outward flow and solvent evaporation. According to the rheological investigation, the solution was a Newtonian fluid up to the concentration of 10% w/v (a critical concentration). The rate of the film thinning is then given by

$$\left(\frac{\mathrm{d}h}{\mathrm{d}t}\right)_1 = -\frac{2\rho_s\omega^2h^3}{3\eta_s(t)} - (E_v)_1, \tag{1}$$

where h is a liquid film thickness, t is a spinning time, ω is a spinning speed, ρ_s is a solution density, $\eta_s(t)$ is a solution viscosity at time t, E_v is an evaporation rate, and subscript 1 denotes the first stage.

At this stage, a constant evaporation rate, E_v, was assumed since the film is so thin and the mass transfer coefficient used here is gas-side controlled as (Perry et al., 1984)

$$(E_v)_1 = k'_G(p_i - p_\infty) = k_G(c_i - c_\infty), \tag{2}$$

where k'_G and k_G are gas-phase mass-transfer coefficients in units of pressure and concentration, respectively, p_i and c_i are partial pressure and concentration, respectively, of solvent vapour at the liquid–gas interface, and p_∞ and c_∞ are partial pressure and concentration, respectively, of the solvent vapour in the atmosphere above the interface. The model can be applied to two cases, i.e. a spinning in an atmosphere (without GYRSET) and a spinning in a confined volume (with GYRSET). The values of p_∞ and c_∞ are equal to zero if the spinning is done in the atmosphere, whereas they increase from zero to saturated pressure or concentration if the spinning is done in the confined volume.

For the case of a spinning disk, the gas-phase mass-transfer coefficient, k_G, can be described as (Middleman, 1998)

$$k_G = 0.62D_{AB}\left(\frac{\rho_a\omega}{\eta_a}\right)^{1/2}\left(\frac{\eta_a}{\rho_a D_{AB}}\right)^{1/3} \tag{3}$$

where D_{AB} is a binary diffusion coefficient of xylene vapour and air, ρ_a is the density of air, and η_a is the viscosity of air.

As the solvent is lost by evaporation, the solution concentration increases and hence, the solution viscosity increases. The relationship between the concentration and viscosity obtained from the rheological study was included into the model. The second stage began once the concentration increases to a point where the polymer precipitates from the solution due to its low solubility in the solvent (around 10% w/v). At this stage, the film could no longer flow by a viscous mechanism and only the quiescent solvent evaporation occurred. The final film thickness was hence calculated on the assumption that all solvent had evaporated from the film (see more details in Yimsiri et al., 2001; Yimsiri, 2002).

The experimental data was compared with three models, namely Emslie's, Meyerhofer's and the modified models. The basis of Emslie's model assumes a constant viscosity and assumes all solvent evaporates after spinning. Fig. 8 shows that Emslie's model substantially underpredicts for the spinning

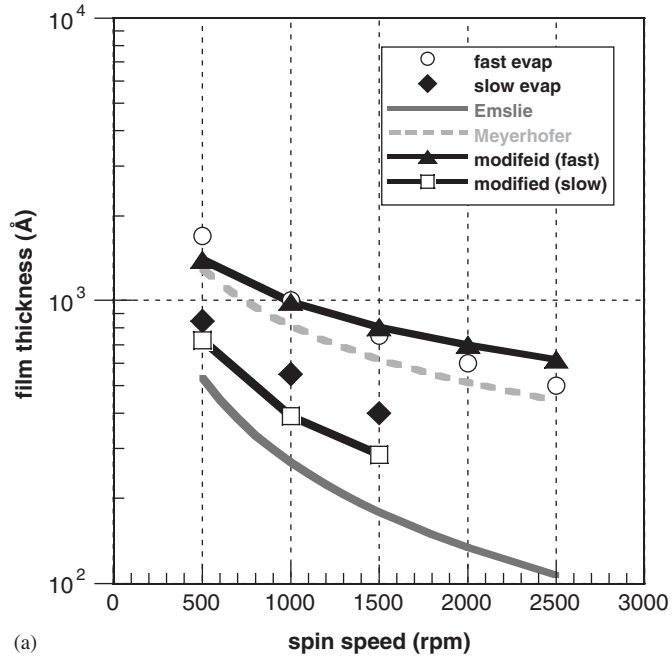

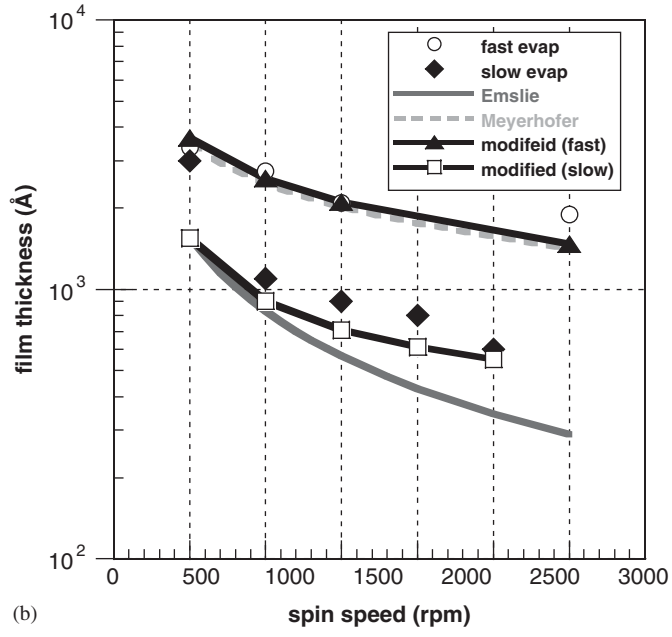

Fig. 8. Comparison between experimental results and model predictions: solution 1 and (b) solution 2.

without the GYRSET (fast evaporation) and are closer to the results for the spinning with the GYRSET (slow evaporation). These findings confirm the strong effects of the solvent evaporation during the spinning. On the other hand, the results from Meyerhofer's model only slightly underpredicts for the spinning without the GYRSET. The underprediction of Meyerhofer's model is due to the fact that the model assumes no solvent evaporation during the initial stage. Conversely, the modified model shows good agreement with the experimental results for both fast and slow solvent evaporation. In general,

Table 2
Value of exponent b obtained experimentally and from the model prediction

Solution	Exponent b			
	Experiment		Modified model	
	With GYRSET	Without GYRSET	With GYRSET	Without GYRSET
1	0.68	0.75	0.85	0.50
2	0.94	0.41	0.65	0.50

the modified model for fast evaporation matches very well with the experimental results, whereas the modified model for slow evaporation slightly underestimates the film thickness.

According to previous studies, the correlation between film thickness and spin speed is typically expressed as a power-law function, $h \propto \omega^{-b}$. The value of the exponent b is dependent on spin-coating fluids if it was found experimentally and on assumptions used if it was found theoretically. In the case of no solvent evaporation, according to Emslie's analysis it was found that the exponent b is equal to 1. The exponent b found from experimental results of Givens and Daughton (1979) for a high-viscosity fluid and from Skrobis et al. (1990) for a solution with low volatility is close to 1, supporting Emslie's theory. If solvent evaporation occurs during the spinning due to the volatility of solvents, several researchers have found the exponent b close to 0.5 (see, for example, Meyerhofer, 1978; Ohara et al., 1989; Skrobis et al., 1990).

The exponent b found experimentally and from the modified models are shown in Table 2 and agree with previous findings, which is, in the case of slow evaporation the exponent b is close to 1. The prediction of the model also shows a decrease of b values as the solution concentration (or viscosity) increases. This is because as mentioned earlier that a high concentration or viscosity solution (solution 2) reaches a plateau thickness at a lower spin speed, resulting in a smaller b compared to that of a low-viscosity solution (solution 1). However, the values of b obtained experimentally are in the opposite direction. This is because a smaller number of data points for solution 1. For fast evaporation, the modified model resulted in a value of 0.5, which is similar to previous studies, whereas the experiments found b to be in the range of 0.4–0.7.

6. Experimental procedure: dip coating

A Stable Microsystems Texture Analyser (TA-XT2) (Stable Microsystems, 1996) was used in the experiment for the dip-coating process. The apparatus is a micro-testing machine normally used for food and pharmaceutical applications. The instrument can move a test probe vertically at a constant speed of between 0.1 and 10 mm/s. The probe has been modified to handle plate substrates. Two sizes of solution baths were used for two sizes of substrates, 25×25 and 50×50 mm^2. A lid with a small slot, for a substrate to be immersed and withdrawn from the bath, was employed to prevent solvent evaporation from the surface of the solution.

Tests were performed on the same type of polymer solutions used for the spin-coating process. The cleaned ITO-coated glass substrate was immersed into the solution bath at a constant dipping speed of 2 mm/s and kept inside the bath for 30 s. The substrate was then withdrawn from the bath at a prescribed withdrawal speed. The film was left to dry and its thickness and uniformity evaluated.

Two drying methods were applied to the polymer films, i.e. ambient drying and hot-air drying, in order to investigate the effect of solvent evaporation. For ambient drying, the substrate was left in a vertical orientation in a fume cupboard for 60 min to dry. For hot-air drying, hot air from a hair dryer was blown onto the substrate during the withdrawal process. A diffuser was attached to the head of the hair dryer to achieve uniform distribution of the hot air. The hot air had a temperature of around 50–60 °C and the blowing speed was approximately 6 m/s. The aim of hot-air drying is to minimise the overlap between the liquid draining and film drying stages, which can cause a non-uniform film thickness. In the following discussion, the ambient drying and hot-air drying are referred to as slow and fast drying, respectively.

7. Dip-coating experimental results

Fig. 9 shows a plot of film thickness, h, as a function of withdrawal speed, u_o solvent evaporation rate, and polymer concentration. The film thickness increases as the withdrawal speed increases. This is because a viscous drag of the moving substrate is proportional to the withdrawal speed. At a higher withdrawal speed, a larger force results in a greater amount of the liquid moving upwards with the substrate, and hence a thicker film. The relationship between the film thickness and the withdrawal speed can be described as $h \propto u_o^x$. The exponent x of both slow and fast drying ranges between 0.4 and 0.6, which agrees with the prediction by Landau and Levich (1942). In addition, the evaporation rate has a minor effect on the film thickness because the film thickness for slow and fast drying is similar. This is due to the fact that an amount of liquid pulled up with the substrate is small, and hence very little of it drains back to the solution bath. For a high concentration (solution 2), thicker films were obtained from the hot-air drying at high withdrawal speeds (2 and 5 mm/s). This is because a high concentration at a high withdrawal speed results in reasonably large amounts of entrained and draining liquid. The hot air prevents the liquid draining, thus a thicker film is achieved. Guglielmi and Zenezini (1990) investigated the effect of the evaporation rate on the thickness of sol–gel coating and found that thinner coating was obtained when the process was carried out in a saturated solvent vapour atmosphere.

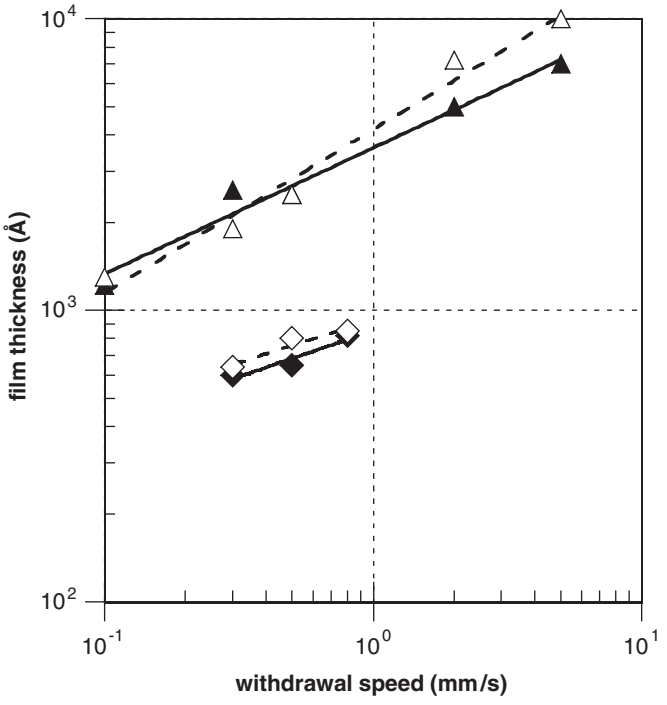

Fig. 9. Film thickness as a function of withdrawal speed. Hot-air drying: (◇) solution 1 ($x = 0.24$) and (△) solution 2 ($x = 0.56$). Ambient drying: (◆) solution 1 ($x = 0.62$) and (▲) solution 2 ($x = 0.43$). Continuous lines: power-law fitting.

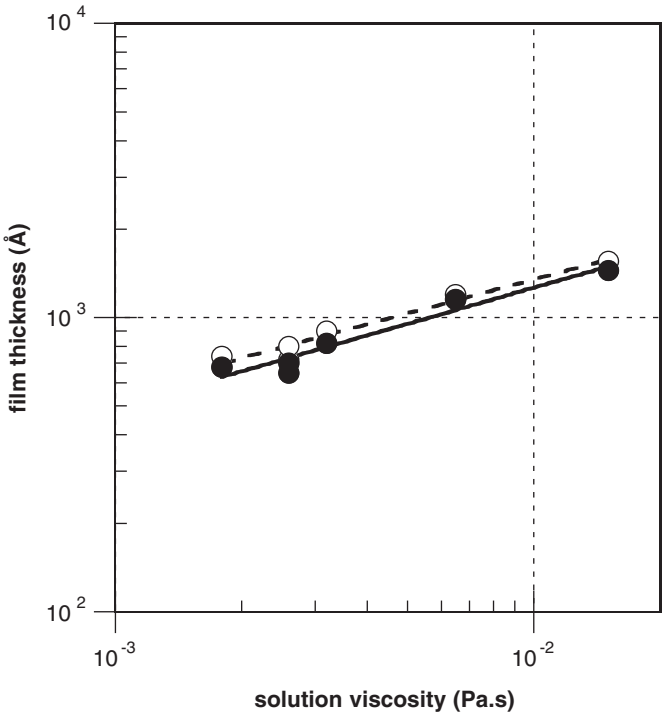

Fig. 10. Effect of initial solution viscosity on film thickness (withdrawal speed of 0.5 mm/s): (●) ambient drying and (○) hot-air drying. Continuous and broken lines: trend lines.

Fig. 10 shows a plot of film thickness as a function of solution viscosity for both slow and fast drying at the withdrawal speed of 0.5 mm/s. In both cases, a solution with a higher viscosity results in a thicker film. This is because at the same withdrawal speed, the amount of the liquid moving upwards with the substrate is larger for a more viscous liquid since the drag force (ηu_o) is proportional to the solution viscosity. Strawbridge and James (1986) also reported the effect of solution viscosity on the film thickness; however, in their experiments,

the change in viscosity was controlled by the change of concentration. Therefore, the thickness dependency found by them was from a combination of both viscosity and concentration.

8. Modelling of dip-coating process

The dip-coating process involves immersing a substrate into a reservoir of solution for sufficient time, to ensure that the substrate is completely wetted, and the withdrawing the substrate from the solution bath (see Fig. 11) (Landau and Levich, 1942). After the solvent has evaporated, a uniform solid film is deposited upon the surface of the substrate. Several forces are involved in the film deposition. The major forces are viscous drag, gravitational force, capillary force (resultant force of surface tension), and inertia force (Schunk et al., 1997). The viscous drag is the force moving liquid upward with the substrate and is proportional to liquid viscosity and withdrawal speed. Gravity acts to drive the liquid downwards. Surface curvature induced by surface tension at the base of the fluid capillary force lowers the pressure in the liquid beneath the curved meniscus near the solution bath and produces a driving force in the same direction as gravity.

A dip-coating analysis was first presented by Landau and Levich (1942). This analysis has subsequently been reviewed widely (e.g. Deryagin and Levi, 1959). The model derivation was based purely on the hydrodynamics of a Newtonian fluid flow, ignoring solvent evaporation. The model considered a case of low velocity of an infinite moving plate and relatively large liquid container (no edge effect). The liquid surface is separated into two independent regions, i.e. (i) the region of the surface situated high above the meniscus and directly dragged by the plate, where the surface of the liquid may be taken to be nearly parallel to the plate surface, and (ii) the region of the meniscus of liquid, which is slightly deformed by the motion of the plate, hence the shape of the surface nearly coincides with the shape of a static meniscus. By using the classical lubrication equations, a matching condition for the film entrainment and the static meniscus regions can be identified and used to obtain an expression for the film thickness as shown in Eq. (9).

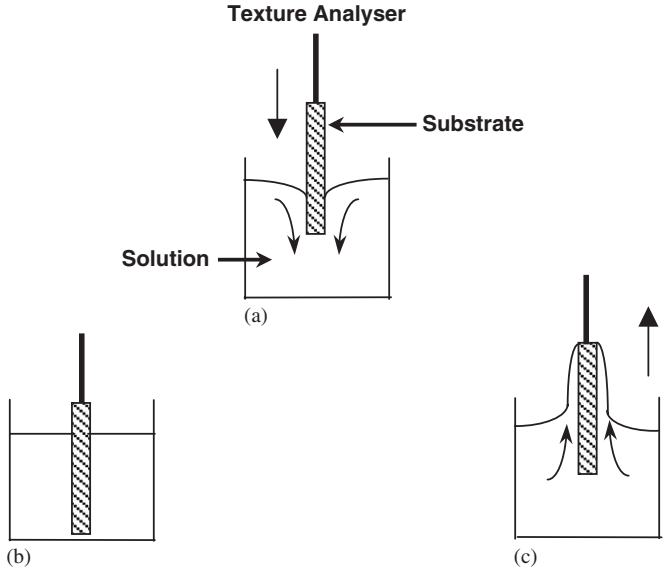

Fig. 11. Schematic diagram of dip-coating process: (a) immersion, (b) wetting, and (c) withdrawal.

$$h_o = 0.944\,\frac{(\eta u_o)^{2/3}}{\sigma^{1/6}(\rho g)^{1/2}} = 0.944(\mathrm{Ca})^{1/6}\left(\frac{\eta u_o}{\rho g}\right)^{1/2}, \tag{9}$$

where h_o is the limiting film thickness, u_o is the withdrawal speed, η is the solution viscosity, ρ is the solution density, σ is the solution surface tension, and Ca ($=\eta u_o/\sigma$) is a capillary number.

The withdrawal speed is the most common parameter used to control the film thickness. There have been a large number of researchers studying the film thickness dependency on the withdrawal speed. The relationship between the film thickness and withdrawal speed can be estimated by a power law of the form $h \propto u_o^x$ (e.g. Landau and Levich, 1942). A wide range of the values of x found experimentally has been reported by various authors, e.g. $x = 0.5$ (Yang et al., 1980; Gibson et al., 1985; Strawbridge and James, 1986), $x=0.67$ (Schroeder, 1969; Dislich and Hussman, 1981), $x = 0.53$–0.64 (Brinker et al., 1991), and $x = 1.0$ (Orgaz and Rawson, 1986). On the other hand, Gao et al. (1995) reported that the film thickness was nearly independent of the withdrawal speed ($x \approx 0$) for very low concentrations (0.001–0.01%) of perfluoropolyester lubricant liquid. The difference in the value of x depends on the solution properties and process conditions. Smaller values of x suggest a weaker film thickness dependency on the withdrawal speed.

Incorporating the effect of solvent evaporation into existing models is mathematically demanding. The model used in this paper modified the Landau and Levich's model (denoted as L&L) by using an arbitrary viscosity of the solution in the solution bath which then increased further due to the effect of solvent evaporation. The modified model is denoted as, for example, 2.7 L&L which means that the viscosity is increased by 2.7 times of the initial value. A multiplying factor for the viscosity depends on solution properties and withdrawal speeds and it was found that the multiplying factor is large at slow withdrawal speeds and decreases as the speed increases. This is because at slow withdrawal speeds, the film is exposed to solvent evaporation at the liquid meniscus for a longer time. On the other hand, fast withdrawal speeds quickly move the substrate from the solution bath and hence, the solvent evaporation at the liquid surface is minimised.

Fig. 12 shows that even though the model of Landau and Levich (1942) fails to quantitatively predict the experimental results, the prediction of the dependency of the withdrawal speed on the film thickness agrees qualitatively with the experimental results. The model suggests that the film thickness, h, varies with the withdrawal speeds, u_o, as a function of $h \propto u_o^{0.67}$, whereas the experimental results show that $h \propto u_o^x$ where x is in the range of 0.4–0.6. This shows a strong influence of the withdrawal speed on the film thickness. It can also be seen that the initial and arbitrary viscosities provide

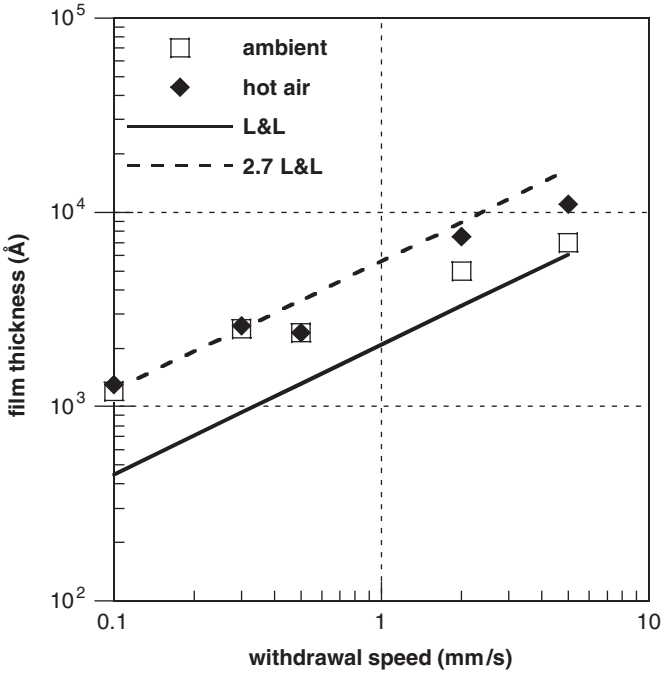

Fig. 12. Comparison between experimental results and model predictions.

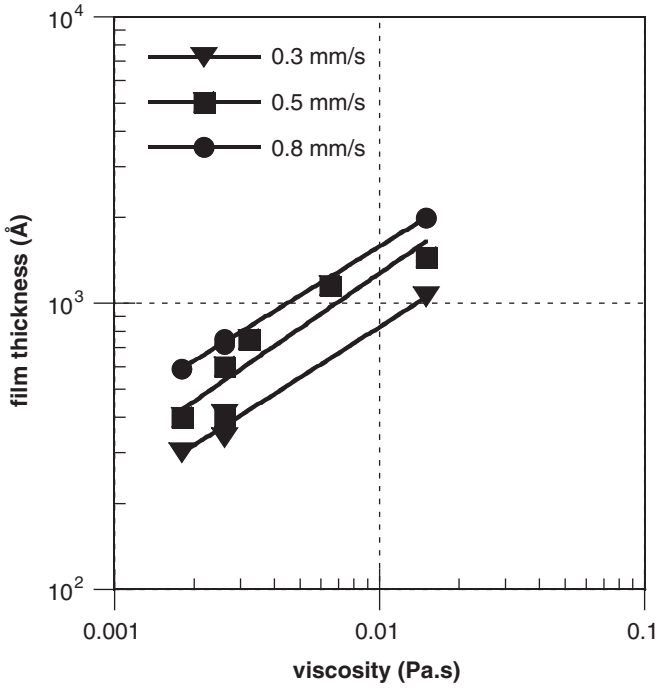

Fig. 13. Film thickness as a function of solution viscosity at different withdrawal speeds for ambient drying.

the upper and lower bounds, respectively, of the experimental results.

The solution properties also play an important role in controlling the film thickness. According to the model of Landau and Levich (1942), the effect of the solution viscosity on the film thickness is as significant as the effect of the withdrawal speed, which can be described by $h \propto (u_o \eta)^{0.67}$.

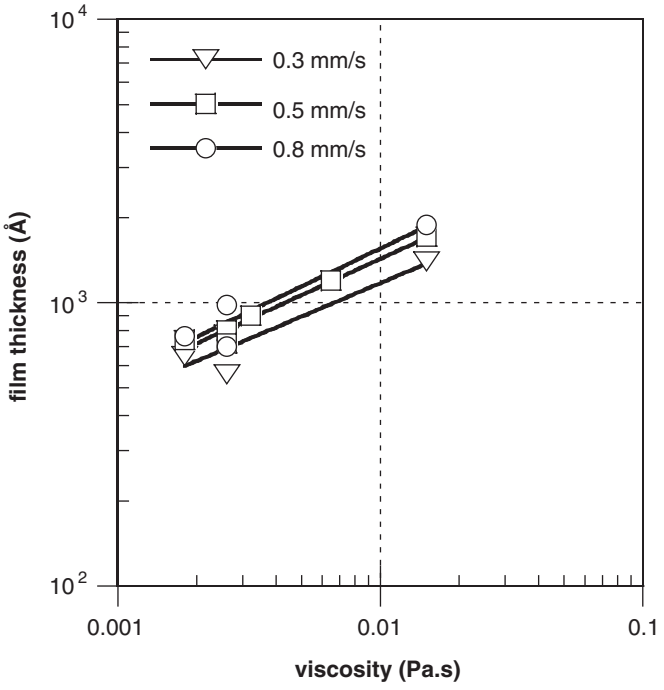

Fig. 14. Film thickness as a function of solution viscosity at different withdrawal speeds for hot-air drying.

Figs. 13 and 14 show plots of film thickness as a function of solution viscosity at different withdrawal speeds for slow and fast drying, respectively. The continuous lines in the figure are the best-fit lines of the experimental results. The results for slow drying reveal a good agreement with the model prediction in which $h \propto \eta^y$ where y is around 0.6. Lower values of the exponent (0.40–0.44) were found in the case of fast drying. For fast drying, the solvent evaporation may occur at the surface of the solution bath and the solution viscosity and the viscosity dependency (power-law exponent) may be affected.

9. Conclusion

This paper has shown that spin and dip coating of LEP solutions is particularly sensitive to the evaporation rate of the solvents during the processing and two models have been used that are able to predict the observed trends. In terms of spin coating, both spin speed and solvent evaporation rate are the key parameters that affect the final film thickness. Both can be externally controlled and a high level of precision obtained in relation to thickness control. A further important aspect; namely the uniformity of the thickness has not been addressed in this paper and this property will be influenced by additional factors such as sample volume and local evaporation conditions.

This paper also shows that dip coating is a viable way of producing thin films of LEP. Dip coating has certain advantages in that the geometry of the substrate does not have to be flat, i.e. it is possible for example to dip-coat rods if required. The dip-coating process can provide similar film thickness control to spin-coating process and also the evaporation process is essentially decoupled from the film-forming process in contrast

to spin coating where film forming and evaporation simultaneously occur.

Acknowledgements

This project was financially supported by the Cambridge Display Technology (CDT) and we would like to thank them for their assistance. In particular, we would like to thank Dr.Illaria Grizzi and Dr. Carl Towns for suggestions and helpful guidance.

References

Braun, D., Heeger, A.J., 1991. Visible light emission from semiconducting polymer diodes. Applied Physics Letters 58 (18), 1982–1984.

Brinker, C.J., Hurd, A.J., 1994. Fundamentals of sol–gel dip-coating. Journal de Physique III 4, 1231–1242.

Brinker, C.J., Frye, G.C., Hurd, A.J., Ashley, C.S., 1991. Fundamentals of sol–gel dip coating. Thin Solid Films 201, 97–108.

Burroughes, J.H., Bradley, D.D.C., Brown, A.R., Marks, R.N., Mackay, K., Friend, R.H., Burns, P.L., Holmes, A.B., 1990. Light-emitting diodes based on conjugated polymers. Nature 347, 539–541.

Carter, J.C., Grizzi, I., Heeks, S.K., Lacey, D.J., Latham, S.G., May, P.G., del los Paños, O.R., Pichler, K., Towns, C.R., Wittmann, H.F., 1997. Operating stability of light-emitting polymer diodes based on poly(p-phenylene vinylene). Applied Physics Letters 71 (1), 34–36.

Chou, H.L., Hsu, S.Y., Weit, P.K., 2005. Light emission in phase separated conjugated and non-conjugated polymer blends. Polymer 46, 4967–4970.

Damon, G.F., 1966. The effect of whirler acceleration on the properties of the photoresist film. In: Proceedings of Kodak Seminar on Microminiaturization, Rochester, pp. 36–43.

Daughton, W.J., O'Hagen, P., Givens, F.L., 1978. Thickness variance of pun-on photoresist, revisited. In: Proceedings of Kodak Seminar on Microelectronics, San Diego, pp. 15–20.

Deryagin, S.M., Levi, S.M., 1959. Film Coating Theory. The Focal Press, London.

Dislich, H., Hussman, E., 1981. Amorphous and crystalline dip coatings obtained from organometallic solutions—procedures, chemical processes and products. Thin Solid Films 77, 129–139.

Emslie, A.G., Bonner, F.T., Peck, L.G., 1958. Flow of a viscous liquid on a rotating disk. Journal of Applied Physics 29 (5), 858–862.

Extrand, C.W., 1994. Spin coating of very thin polymer films. Polymer Engineering and Science 34 (5), 390–394.

Friend, R.H., Gymer, R.W., Holmes, A.B., Burroughes, J.H., Marks, R.N., Taliani, G., Bradley, D.D.C., Dos Santos, D.A., Brédas, J.L., Lögdlund, M., Salaneck, W.R., 1999. Electroluminescence in conjugated polymers. Nature 397, 121–128.

Gao, C., Lee, Y.C., Chao, J., Russak, M., 1995. Dip-coating of ultra-thin liquid lubricant and its control for thin-film magnetic hard disks. IEEE Transactions on Magnetics 31 (6), 2982–2984.

Gibson, M., Frejlich, J., Machorro, R., 1985. Dip-coating method for fabricating thin photoresist films. Thin Solid Films 128, 161–170.

Givens, F.L., Daughton, W.J., 1979. On the uniformity of thin films: a new technique applied to polyimides. Journal of Electrochemistry Society 126 (2), 269–272.

Guglielmi, M., Zenezini, S., 1990. The thickness of sol–gel silica coating obtained by dipping. Journal of Non-Crystalline Solids 121, 303–309.

Gupta, S.A., Gupta, R.K., 1998. A parametric study of spin coating over topography. Industrial and Engineering Chemistry Research 37, 2223–2227.

Hall, D.B., Underhill, P., Torkelson, J.M., 1998. Spin coating of thin and ultrathin polymer films. Polymer Engineering and Science 38 (12), 2039–2045.

Janietz, S., Bradley, D.D.C., Grell, M., Giebeler, C., Inbasekaran, M., Woo, E.P., 1998. Electrochemical determination of the ionization potential and electron affinity of poly(9,9-dioctylfluorene). Applied Physics Letters 73 (17), 2453–2455.

Kim, J.S., Friend, R.H., Cacialli, F., 1999. Improved operational stability of polyfluorene-based organic light-emitting diodes with plasma-treated indium-tin-oxide anodes. Applied Physics Letters 74 (21), 3084–3086.

Landau, L., Levich, B., 1942. Dragging of a liquid by a moving plate. Acta Physicochimica U.R.S.S. 17 (1–2), 42–54.

Larson, R.G., Rehg, T.J., 1997. Spin coating. In: Kistler, S.F., Schweizer, P.M. (Eds.), Liquid Film Coating: Scientific Principles and Their Technological Implications. Chapman & Hall, London, pp. 673–708.

Macosko, C.W., 1994. Rheology: Principles, Measurements, and Applications. Wiley-VCH, New York.

Mentley, D.E., 2002. State of flat-panel display technology and future trends. Proceedings of IEEE 90 (4), 453–459.

Meyerhofer, D., 1978. Characteristics of resist films produced by spinning. Journal of Applied Physics 49 (7), 3993–3997.

Middleman, D., 1998. An Introduction to Mass and Heat Transfer: Principles of Analysis and Design. Wiley, New York.

Ohara, T., Matsumoto, Y., Ohashi, H., 1989. The film formation dynamics in spin coating. Physics Fluids A 1 (12), 1949–1959.

Orgaz, F., Rawson, H., 1986. Coloured coating prepared by the sol–gel process. Journal of Non-Crystalline Solids 82, 378–390.

Perry, R.H., Green, D.W., Maloney, J.O., 1984. Perry's Chemical Engineers' Handbook. McGraw-Hill, New York.

Redecker, M., Bradley, D.D.C., Inbasekaran, M., Woo, E.P., 1998. Nondispersive hole transport in an electroluminescent polyfluorene. Applied Physics Letters 79 (11), 1565–1567.

Sapp, S.A., Sotzing, G.A., Reynolds, J.R., 1998. High contrast ratio and fast-switching dual polymer electrochromic devices. Chemistry of Materials 10 (8), 2101–2108.

Schroeder, H., 1969. Oxide layers deposited from organic solutions. In: Hass, G., Thun, R.E. (Eds.), Physics of Thin Films, vol. 5. Academic Press, New York, pp. 87–141.

Schunk, P.R., Hurd, A.J., Briker, C.J., 1997. Free-meniscus coating processes. In: Kistler, S.F., Schweizer, P.M. (Eds.), Liquid Film Coating: Scientific Principles and Their Technological Implications. Chapman & Hall, London, pp. 673–708.

Schwartz, G.C., 1965. Thickness studies on exposed kodak thin film resist films. In: Proceedings of Kodak Seminar on Microminiaturization, Rochester, pp. 41–48.

Scriven, L.E., 1988. Physics and applications of dip coating and spin coating. Materials Research Society Symposium Proceedings 121, 717–729.

Skrobis, K.J., Denton, D.D., Skrobis, A.V., 1990. Effect of early solvent evaporation on the mechanism of the spin-coating of polymeric solutions. Polymer Engineering and Science 30 (3), 193–196.

Stable Microsystems, 1996. Company's manuscript.

Stevens, M.A., Silva, C., Russell, D.M., Friend, R.H., 2001. Exciton dissociation mechanisms in the polymeric semiconductirs poly(9,9-dioctylfluorene) and poly(9,9-dioctylfluorene-co-benzothiadiazole). Physics Review B 63 (16), 165213.

Strawbridge, I., James, P.F., 1986. The factors affecting the thickness of sol–gel derived silica coating prepared by dipping. Journal of Non-Crystalline Solids 86 (3), 381–393.

Weill, A., Dechenaux, E., 1988. The spin-coating process mechanism related to polymer solution properties. Polymer Engineering and Science 28 (5), 945–948.

Wu, C.C., Wu, C.I., Sturm, J.C., Kahm, A., 1997. Surface modification of indium tin oxide by plasma treatment: an effective method to improve the efficiency, brightness, and reliability of organic light emitting devices. Applied Physics Letters 70 (11), 1348–1350.

Yang, C.-C., Josefowicz, J.Y., Alexandru, L., 1980. Deposition of ultrathin films by a withdrawal method. Thin Solid Films 74 (1), 117–127.

Yimsiri, P., 2002. The processing of light emitting polymer solutions. Ph.D Thesis, University of Cambridge, UK.

Yimsiri, P., Mackley, M.R., Lele, A., Grizzi, I., Towns, C.R., 2001. The spin coating of thin light emitting polymers. In: Proceedings of Sixth World Congress of Chemical Engineering, Melbourne, Australia.